Textile Loop Antenna and TFT Channel-Select Circuit for Fully Bendable TFT Receivers

T. Meister, K. Ishida, R. Shabanpour, B. Kheradmand-Boroujeni, C. Carta, F. Ellinger
Technische Universität Dresden
Dresden, Germany

***Abstract*—In this paper we present the design, measurements, simulation, and modelling of a flexible textile loop antenna. Using embroidering techniques, a stranded copper wire is integrated onto a textile substrate, which in turn can be part of a garment or wearable accessory. The targeted application is a textile antenna integrated into the sides of a messenger bag next to fully flexible a-IGZO TFT receiver circuitry. The carrier frequency is dictated by the relatively slow TFTs, which limit the operation frequency of the receiver. As a result, a compact antenna for frequencies in the range of 100 kHz to 10 MHz is required. For this purpose loop antennas are suited. They usually provide only a limited gain, yet they allow for a low profile. Since the performance of thin and organic large area electronics (TOLAE) technologies improves steadily, we also investigate their applicability for higher carrier frequencies, which will enable smaller antenna dimensions. Finally we present a fully flexible TFT circuit to tune the antenna characteristics.**

Keywords—Textile antenna, wearable antenna, inductor, electromagnetic simulation, modeling, bendable electronics.

I. INTRODUCTION

While improvements in the performance of electronics are typically measured in switching speed, power consumption, gain, and so on, full bendability is a comparatively new feature of electronics, which opens attractive fields of applications. Bendable electronics can be applied to curved surfaces or integrated into garments and accessories, while usually being at the same time ultra-thin. To go along with bendable electronics and to allow integration of full wireless systems, flexible antennas are also required. This, however, poses the challenge of changing antenna characteristics, because of varying geometries as well as the varying proximity to bodies.

Textile and wearable antennas have been proposed for various fields of application such as military [1], medical [2], and RFIDs [3, 4]. Also, consumer wearable antennas for wireless communication [5] have been presented. Such a textile antenna can for example use a copper foil as well as conductive threads [1], or it can be printed using conductive polymers [6]. Such an antenna structure has to be very robust, because it will be bent back and forth frequently. Also, if integrated in a garment, such an antenna has to withstand washing cycles.

While the wireless system targeted in this work requires carrier frequencies below 10 MHz, previous works focus on small antennas for frequencies of 500 MHz or above. This high frequency range allows for small antenna dimensions and enables many kinds of integration. However, the high carrier frequencies cannot be used for wireless systems that rely on the emerging bendable *thin and organic large area electronics* (TOLAE) technologies. Instead conventional rigid electronics are required. However, those conventional electronics cannot be easily integrated in the same way as a textile antenna.

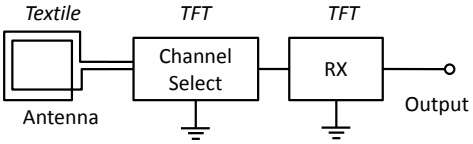

Fig. 1. System architecture of the target OOK-receiver (RX).

We aim at developing a fully flexible on-off keying (OOK) receiver in a bendable thin-film transistor (TFT) technology with a low data rate. The basic system architecture of the fully flexible receiver is shown in Fig. 1. Its dimensions and bendability enable the integration of the receiver, including its antenna, for example into a messenger bag. It will allow a transmitter to remotely trigger several actions in the bag. The range will be tens of meters. A suitable receiver circuit in an amorphous indium gallium zinc oxide (a-IGZO) TFT technology is presented in [7].

Bendable electronics have low maximum frequencies of operation compared to conventional electronics. A peak transit frequency f_t of 135 MHz [8] and an amplifier with a gain-bandwidth product of 6.4 MHz [9] was reported for an available a-IGZO TFT technology. That means wireless communication systems with a carrier frequency of up to a few MHz can be realized. Therefore, in this work we aim at designing the textile antenna to allow carrier frequencies in the range from 100 kHz to 10 MHz.

To achieve a low profile in spite of the targeted frequency range, we chose a loop antenna. The performance of bendable electronics technologies will certainly be improved steadily. As a consequence we also investigate the usability of our proposed antenna for higher carrier frequencies, which will allow for longer communication distances and/or smaller antenna dimensions. Finally we will demonstrate how a bendable a-IGZO TFT channel-select circuit can be used to tune the antenna characteristics.

 DOI: 10.1109/IMOC.2015.7369131.

II. Textile Antenna

A. Materials and Layout

The antenna substrate is a poly-cotton blended fabric that can have a polyurethane (PU) membrane transferred to one of its sides. This PU membrane increases the stability and durability of the textile. However, the membrane is not comfortable when worn directly on the skin. The electrical conductor is a stranded copper wire with 34 filaments of 50 µm diameter each. This wire was chosen because of its low resistivity and usability at 10 MHz. The skin depth in the targeted frequency range is above 15 µm and affects the effective resistance by less than 15 %. Therefore, in the remainder of this work we will not consider it further. The characteristics of the wire are shown in Table I. The wire is embroidered onto the substrate as shown in Fig. 2. The upper yarn is a transparent nylon thread, which optically exposes the stranded copper wire; the lower yarn is in polyester. Down to a pitch of 2 mm of the embroidered wire it can be assured that there is no short circuit between adjoining wires. Consequently, in this work we assumed the minimum allowable pitch to be 2 mm. However, since each filament of the used copper wire is individually coated, a smaller pitch or embroidering two wires on top of each other are available options. Assuming the outer dimensions remain the same, this would improve the antenna performance over the results presented here. Yet, the durability of the antenna may be affected because of abrasion of the coating.

The layout of the embroidered wire for the textile loop antenna is shown in Fig. 3. All parts of the embroidery, including the cross-over on the left, can be done on the same side of the textile without creating shorts, because the strands of the wire are coated. A main goal of this work was to allow integration into a messenger bag. For this purpose the outer dimensions of width W = 25.5 cm and length L = 35.5 cm were chosen for the antenna. The three different combinations of number of turns N and pitch p, which are listed in Table II, were investigated. All the listed configurations were designed, fabricated and tested.

B. Measurements

To measure antenna characteristics we employ a network analyzer to determine the S-parameter S_{11} and finally extract the relevant characteristics. Measurement results for the three flat antenna samples are listed in Table III. The real parts of their impedances are plotted in Fig. 4. The influence of bending the antenna along the "length"-axis (ref. Fig. 3a) for antenna sample A10-2 is shown in Fig. 5. Bending the antenna increases the resonance frequency f_c, as expected. This is because bending reduces the effective area of the antenna, which reduces its inductance L and thus increases f_c. This result shows that the antenna characteristics depend on the bending radius considerably. Those variations of the antenna characteristics have to be considered and mitigated by the system design of the receiver.

C. Simulation

To simulate the characteristics of the flat antenna before fabrication, we use a 3-D planar electromagnetic (EM) field solver. The wire is modelled as a solid with a rectangular cross-section of 258 µm x 258 µm, which is equivalent to the actual area of the stranded wire cross-section. Using air as dielectric, the simulation results are shown in Table IV marked with *air* and as the dotted line in Fig. 6. As expected the dc-resistance R_{DC} as well as the inductance L are close to the actual measurement results, while the self-resonance f_c and resistance R_c at the self-resonance frequency differ significantly from the measurement results (compare Table III). This is because the

TABLE I. Characteristics of the stranded copper wire.

Copper Alloy	E-Cu 58
Weight Composition in %	Cu 99.95
	Oxygen 0.005 - 0.040
Resistivity in Ω · m	$1.71 \cdot 10^{-8}$
Resistivity per unit length in Ω / m	0.256
Filaments	34, individually coated
Filament diameter in µm	50
Effective total diameter in µm	292

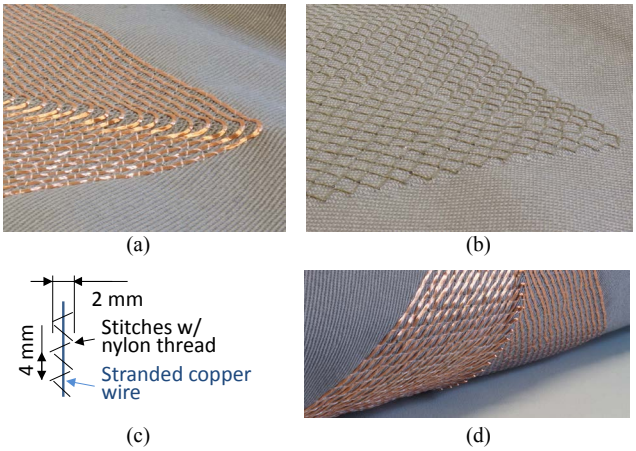

(a) (b) (c) (d)

Fig. 2. (a) Embroidered stranded copper wire using nylon thread, (b) backside of the same cloth, (c) embroidering dimensions, and (d) photo of bent textile antenna.

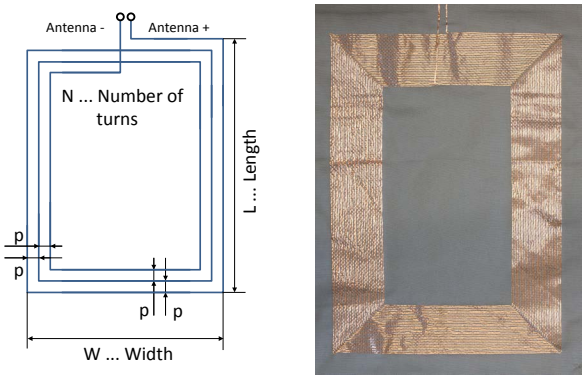

(a) (b)

Fig. 3. (a) Layout of textile loop antenna and (b) photograph of fabricated antenna with N = 30 and p = 2 mm.

TABLE II. Antenna layout parameters for fabrication.

Antenna Sample	*A30-2*	*A10-2*	*A05-5*
L in cm	35.5		
W in cm	25.5		
N	30	10	5
p in mm	2	2	5

TABLE III. ANTENNA MEASUREMENT RESULTS.

Antenna Sample	*A30-2*	*A10-2*	*A05-5*
R_{DC} in Ohm	7.0	2.4	1.3
L in µH (@ f=100kHz)	392	80.0	20.2
f_c in MHz	1.75	4.41	9.00
R_c in kOhm	331.2	103.0	18.3
Maximum Q	85 @620kHz	85 @1.0MHz	65 @1.4MHz

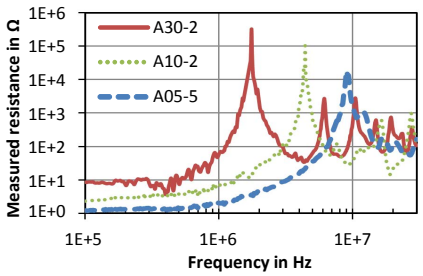

Fig. 4. Measured antenna resistances.

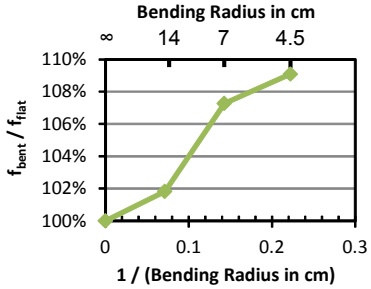

Fig. 5. Effect on f_c of bending antenna A10-2 along its "length"-axis.

model for the EM simulation does not represent capacitances of the antenna structure well. The embroidering process presses the cross-section of the wire flat to varying widths and thicknesses. Due to manufacturing tolerances the wires are not embroidered completely straight. Consequently, the distance of adjacent turns varies along the circumference. These tolerances make it exceedingly difficult to precisely model the antenna when using a physically correct EM simulation setup.

However, to dramatically improve the prediction accuracy for f_c, we adjust the dielectric constant of the space surrounding the antenna in the EM simulation to fit the measurement results. For this purpose we chose $\varepsilon_r = 18$. The respective results are shown in Fig. 6 and Table IV. As can be seen adjusting ε_r improves the prediction of f_c for all antenna samples alike. However, R_c is still overestimated by a factor of two. Since the value of R_c is less relevant during the design of the antenna layout, this is acceptable.

D. Modeling

For circuit design it is convenient to use a model consisting of few lumped elements to represent the antenna impedance. We model the antenna using the schematic shown in Fig. 7, which results in a modelled antenna impedance of:

$$Z(\omega) = \left(1/_{j\omega \cdot C_{self}} + R_{ra}\right) || (R_{DC} + j\omega \cdot L). \qquad (1)$$

TABLE IV. RESULTS OF EM SIMULATION FOR $\varepsilon_r = 1$ (AIR) AND $\varepsilon_r = 18$.

Antenna Sample	*A30-2*		*A10-2*		*A05-5*	
Simul. Dielectric	air	$\varepsilon_r = 18$	air	$\varepsilon_r = 18$	air	$\varepsilon_r = 18$
$R_{DC\ EM}$ in Ohm	6.4	6.4	2.5	2.5	1.2	1.2
L_{EM} in µH (@ f=100kHz)	18	18	74	76	375	397
$f_{c\ EM}$ in MHz	3.14	2.17	7.21	3.68	17.55	8.75
$R_{c\ EM}$ in kOhm	841	785	289	199	88	46

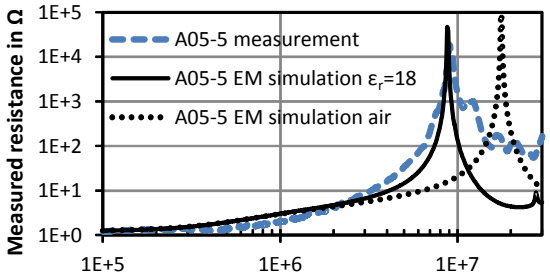

Fig. 6. Simulated antenna resistance of antenna A05-5.

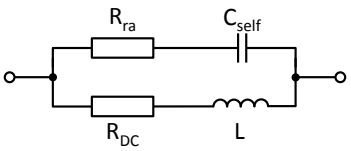

Fig. 7. Antenna model of lumped components.

It models the antenna impedance at frequencies below the second resonance.

The loop antenna will be operated around its first resonance frequency f_c. Therefore, the model is required to be accurate particularly at frequencies close to f_c. The strategy to determine the parameters of the antenna model based on the measured impedance is as follows: a) L is extracted from the measured S-parameters S_{11} at low frequencies (see Table III). b) C_{self} is calculated from the measured resonance frequency f_c and the inductance L as stated in equation (2):

$$C_{self} = \frac{1}{\omega_c^2 \cdot L} \qquad (2)$$

with $\omega_c = 2 \cdot \pi \cdot f_c$. c) For parameter R_{DC} also the measured value is used (see Table III). d) The resistance R_{ra} is calculated such that the modelled antenna resistance $R(\omega) = \text{real}(Z(\omega))$ is equal to the measured antenna resistance R_c at frequency f_c:

$$R_{ra} = R_c + \frac{R_c^2 \cdot (R_{DC} - R_c)}{(\omega_c \cdot L)^2 + (R_{DC} - R_c)^2} \qquad (3)$$

The resulting model parameters for the three antenna samples are listed in Table V. A comparison of the modelled and the measured antenna impedances is shown in Fig. 8.

E. Scaling of Dimensions and Frequency Range

Along with the currently increasing performances of TOLAE technologies, the carrier frequency for wireless communication using flexible electronics of this kind will also increase. Therefore, in this Section we use the simulation

TABLE V. ANTENNA MODEL PARAMETERS.

Antenna Sample	*A30-2*	*A10-2*	*A05-5*
L in µH	392	80.0	20.2
C_{self} in pF	21.1	16.3	15.5
R_{DC} in Ω	7.0	2.4	1.3
R_{ra} in Ω	47.4	45.7	69.7

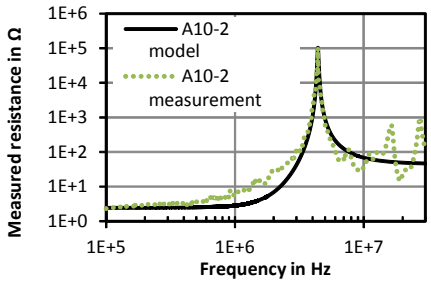

(a)

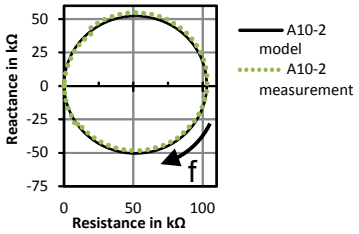

(b)

Fig. 8. Antenna sample A10-2. (a) Comparison of measured and modelled resistances in the frequency range from 100 kHz to 30 MHz. (b) Comparision of measured and modelled impedance in the frequency range from 100 kHz to 10 MHz.

method described in Section II-C to determine characteristics of a smaller antenna layout that is suitable for higher frequencies. We choose three layouts of which the dimensions are shown in Table VI. The first antenna A04-2 is smaller than a credit card, the second is even more compact, and the third has only one turn and as such is a limiting case. Antennas of these dimensions can easily be integrated into garments and accessories in various locations.

The simulation results are listed in Table VI. They indicate that this kind of antenna layout using the before described materials can cover frequencies up to about 400 MHz.

III. A-IGZO TFT CHANNEL SELECT CIRCUIT

We designed and fabricated two versions A and B of a channel selection circuit in the bendable a-IGZO TFT technology described in [10]. Regarding its bendability it could be integrated on the same textile substrate as the loop antenna. The schematic and the die photo of version A are shown in Fig. 9. The circuit can be used to select four different center frequencies. For that purpose it takes a two bit digital input word consisting of bits c1 and c2. Depending on c1 and c2 the capacitive load to the attached textile loop antenna is changed to the values listed Table VII.

For the simulations of the a-IGZO TFTs we use the Rensselaer Polytechnic Institute-amorphous TFT (RPI-aTFT) model [11] fitted to the used a-IGZO technology. The presented results also include the effect of parasitics extracted from the layout. Table VII also shows the capacitances of the

TABLE VI. SIMULATION RESULTS FOR SMALL ANTENNAS.

Antenna Sample	*A04-2*	*A03-2*	*A01-2*
L in cm	7	4	4
W in cm	4	4	4
N	4	3	1
p in mm	2	2	n.a.
Simulation Dielectric	$\varepsilon_r = 18$	$\varepsilon_r = 18$	$\varepsilon_r = 18$
$R_{DC\ EM}$ in Ohm	0.17	0.10	0.03
L_{EM} in µH (@f=100kHz)	1.9	0.9	0.2
$f_{c\ EM}$ in MHz	49.7	88.7	417
$R_{c\ EM}$ in kOhm	91.6	43.2	52.3

second version B of the channel select circuit which implements the layout shown in Fig. 9b twice, which because of parasitics does not precisely present twice the capacitive load. Fig. 10 shows simulation results how version B influences the antenna resistance of sample A30-2 depending on the digital input word. Depending on the input word the frequency f_c changes from originally 1.75 MHz to 484 kHz, 253 kHz, 190 kHz, and 159 kHz respectively. Circuit version A changes frequency f_c to 813 kHz, 376 kHz, 276 kHz, and 230 kHz.

TABLE VII. SIMULATED CAPACITIVE LOAD OF CHANNEL SELECT CIRCUIT DEPENDING ON TWO BIT INPUT WORD.

Input word		**Simulated capacitive load to antenna**	
c1	***c2***	***Circuit version A***	***Circuit version B***
0	0	77 pF	250 pF
0	1	369 pF	826 pF
1	0	684 pF	1455 pF
1	1	987 pF	2059 pF

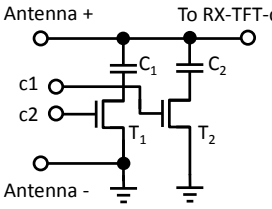

(a)

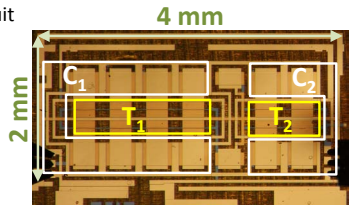

(b)

Fig. 9. Digital channel select circuit (a) schematic and (b) die photo. Transistor dimensions: T_1 (W/L): 8 x 300 µm x 5 µm, T_2: 4 x 300 µm x 5 µm. Capacitances: C_1 = 606 pF, C_2 = 303 pF.

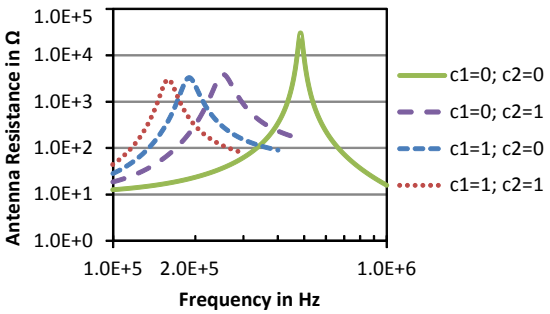

Fig. 10. Effect of the channel select TFT circuit and different digital input words c1,c2 on the antenna resistance of antenna sample A30-2.

IV. Conclusion

In this paper we presented a flexible textile loop antenna for use with wireless receivers in emerging bendable TOLAE technologies. Considering the comparably low frequencies, it has a low profile. Its materials and small size enable its integration into the sides of a messenger bag or garments. It is designed for use with a fully bendable receiver in a-IGZO TFT technology. Since the frequency of operation of this technology, as well as of other emerging TOLAE technologies, are yet comparably low, the targeted frequency range for the antenna was from 100 kHz to 10 MHz. We fabricated three antenna samples with different geometric parameters and showed the respective measurements, simulations, as well as models for circuit simulation. With the developed EM simulations we are able predict that this kind of textile loop antenna could be used up to a frequency of the low hundreds of MHz. We also presented a bendable channel select circuit that was fabricated in a-IGZO TFT technology, which can be used to tune the antenna by a digital control word. Thanks to the bendability of the TFTs it could be integrated on the textile substrate with the antenna.

Acknowledgement

This work was supported in part by the European Commission under project FLEXIBILITY under Grant 287568 and in part by the German Research Foundation within the Cluster of Excellence "Center for Advancing Electronics Dresden–Organic Path". The textile antennas were fabricated by Smartex S.r.l., Pisa, Italy. The TFT channel select circuits were fabricated by the Swiss Federal Institute of Technology, Zurich, Switzerland.

References

[1] P. Salonen, and Y. Rahmat-Samii, "Textile antennas: effects of antenna bending on input matching and impedance bandwidth," *Aerospace and Electronic Systems Magazine, IEEE* , vol.22, no.3, pp.10-14, 2007.

[2] M. A. R. Osman, M. K. Abd Rahim, N. A. Samsuri, H. A. M. Salim, and M. F. Ali, "Embroidered fully textile wearable antenna for medical monitoring applications," *Progress In Electromagnetics Research*, Vol. 117, 321-337, 2011.

[3] L. Vojtech, R. Dahal, D. Mercan, and M. Neruda, "RFID Textile Antenna and Its Development," in *Radio Frequency Identification from System to Applications*, Chapter 9, ISBN 978-953-51-1143-6, 2013

[4] R. Saba, T. Deleruyelle, J. Alarcon, M. Egels, and P. Pannier, "A resistant textile tag antenna for RFID UHF frequency band," *RFID-Technologies and Applications,* pp.203-207, 2012.

[5] Z. Wang; L. Zhang; D. Psychoudakis, and J. L. Volakis, "Flexible textile antennas for body-worn communication," *Antenna Technology (iWAT), 2012 IEEE International Workshop on* , pp.205,208, 5-7 March 2012.

[6] Y. Bayram, Y. Zhou, J. L. Volakis, B.-S. Shim, and N. A. Kotov, "Conductive textiles and polymer-ceramic composites for novel load bearing antennas," *Antennas and Propagation Society International Symposium, 2008. AP-S 2008. IEEE* , pp.1,4, 5-11 2008.

[7] K. Ishida, R. Shabanpour, T. Meister, B. K. Boroujeni, C. Carta, L. Petti, N. Münzenrieder, G. A. Salvatore, G. Tröster, and F. Ellinger, "15 dB Conversion Gain, 20 MHz Carrier Frequency AM Receiver in Flexible a-IGZO TFT Technology with Textile Antennas," *Symposium on VLSI Circuits*, Kyoto, Japan, June 2015. In press.

[8] N. Munzenrieder, L. Petti, C. Zysset, T. Kinkeldei, G. A. Salvatore, and G. Troster, "Flexible Self-Aligned Amorphous InGaZnO Thin-Film Transistors With Submicrometer Channel Length and a Transit Frequency of 135 MHz," *IEEE Transactions on Electron Devices*, vol. 60, no. 9, pp.2815-2820, 2013.

[9] N. Munzenrieder, G. A. Salvatore, L. Petti, C. Zysset, L. Büthe, C. Vogt, G. Cantarella, and G. Tröster, "Contact resistance and overlapping capacitance in flexible sub-micron long oxide thin-film transistors for above 100 MHz operation," *Applied Physics Letters*, vol. 105, no.26, pp.263504, 2014.

[10] N. Munzenrieder, L. Petti, C. Zysset, G. A. Salvatore, T. Kinkeldei, C. Perumal, C. Carta, F. Ellinger, and G. Troster, "Flexible a-IGZO TFT amplifier fabricated on a free standing polyimide foil operating at 1.2 MHz while bent to a radius of 5 mm," *IEEE International Electron Devices Meeting*, pp.5.2.1-5.2.4, 2012.

[11] B. Iniguez, R. Picos, D. Veksler, A. Koudymov, M. S. Shur, T. Ytterdal, and W. Jackson, "Universal compact model for longand short-channel Thin-Film Transistors," *Solid-State Electronics*, vol. 52, pp. 400-405, 2008.